The Cryosphere
Discussions

Open Access

SeaRISE experiment revisited: sources of spread in multi-model projections of the Greenland ice-sheet

F. Saito[1], A. Abe-Ouchi[2,1], K. Takahashi[1], and H. Blatter[3]

[1]Japan Agency for Marine-Earth Science and Technology, Yokohama, Japan
[2]Atmosphere Ocean Research Institute, Univ. of Tokyo, Kashiwa, Japan
[3]Institute for Atmospheric and Climate Science, ETH Zurich, Zurich, Switzerland

Correspondence to: F. Saito (saitofuyuki@jamstec.go.jp)

Discussion Paper | Discussion Paper | Discussion Paper | Discussion Paper

TCD

9, 1383–1424, 2015

SeaRISE revisited

F. Saito et al.

Title Page

Abstract	Introduction
Conclusions	References
Tables	Figures

◀ ▶

◀ ▶

Back Close

Full Screen / Esc

Printer-friendly Version

Interactive Discussion

Abstract

The present paper revisits the future surface-climate experiments of the Greenland ice-sheet proposed by the Sea-level Response to Ice Sheet Evolution (SeaRISE, Bindschadler et al., 2013) study. The projections of the different SeaRISE participants show diversion, which has not been examined in detail to date. A series of sensitivity experiments are conducted and analyzed using the Ice-sheet model for Integrated Earth-system Studies (IcIES) by replacing one or more formulations of the model parameters with those adopted in other model(s). The results show that the main sources of the diversion between the projections of the different SeaRISE participants are differences in the initialization methods and in the surface mass balance methods, and both aspects have almost equal impact on the results. Treatment of ice-sheet margins in the simulation has a secondary impact on the diversion. We conclude that spinning-up the model using fixed topography through the spin-up period while the temperature is allowed to evolve according to the surface temperature history is the preferred representation at least for the experiment configuration examined in the present paper. A benchmark model experiment set-up that most of the numerical model can perform is proposed for future intercomparison projects, in order to evaluate the uncertainties relating to pure ice-sheet model flow characteristics.

1 Introduction

Numerical modeling is an important technique for projecting the response of ice-sheets to climate change (e.g. Huybrechts and de Wolde, 1999). Each of the processes simulated in ice-sheet experiments have a certain degree of uncertainty associated with them, and thus the final output may sometimes have significant diversion among possible combinations of the methods used to represent them. Multi-model intercomparison over a standardized protocol of numerical experiments is a typical approach for evaluating the uncertainties in model projections. Several intercomparison experiments have

Title Page

Abstract | Introduction

Conclusions | References

Tables | Figures

◄ | ►

◄ | ►

Back | Close

Full Screen / Esc

Printer-friendly Version

Interactive Discussion

been previously performed with focus on various topics, in particular on the behavior of the Greenland ice-sheet under future climate changes.

Typical procedures for investigating impact of model parameters on the uncertainties in the short-term projection of Greenland ice-sheet are parameter studies and sensitivity studies using one numerical model (Huybrechts et al., 1991; Huybrechts and de Wolde, 1999; Graversen et al., 2011; Rogozhina et al., 2011; Seddik et al., 2012; Gillet-Chaulet et al., 2012; Yan et al., 2013; Seroussi et al., 2013; Goelzer et al., 2013).

As numerical models have become more and more complex, it has become more difficult to examine the sensitivity to all uncertainties in all possible model formulations, both numerical and physical. Multi-model intercomparison is, although not perfect, an effective procedure for evaluation of model uncertainties. Greve and Herzfeld (2013) performed sensitivity studies of 500 year projections of the Greenland ice-sheet under two scenarios, the AR4 climate scenario and doubled basal sliding, using two different numerical ice-sheet models. Both models differ not only in the numerical and physical representation of ice-sheet dynamics, but also in the method used to compute the surface mass balance from surface temperatures. Despite the differences, a common result is obtained, showing a larger sensitivity to climate warming than to a doubling of the basal sliding. Herzfeld et al. (2012) studied the sensitivity of Greenland ice-sheet projections to the regional updating of the bedrock topography for some glaciers, also using two different numerical ice-sheet models. Both models show significant impact on the response to the doubled sliding scenario by just changing some limited area of bedrock topography. Shannon et al. (2013) use four numerical ice-sheet models to evaluate the effect of enhanced basal sliding driven by surface runoff on 200 years of evolution of the Greenland ice-sheet. Edwards et al. (2014) use six numerical ice-sheet models to evaluate three types of modeling uncertainties: climate model input, ice-sheet model choice, and the interaction of the two systems in terms of the surface mass balance-elevation feedback. While some common features from these papers can be extracted, some divergence in the results seems to be unavoidable.

SeaRISE (Sea-level Response to Ice Sheet Evolution) is a multi-model community effort to investigate the likely range of the evolution of the Greenland and Antarctic ice-sheets over the next few hundred years (Bindschadler et al., 2013). A total of eight models were participants for the Greenland experiments (Nowicki et al., 2013). A series of century-scale sensitivity experiments to prescribed changes of surface climate, sub-ice-shelf melting, and basal sliding were performed. The results exhibit a large range in projected changes for the ice-sheet volume changes: projected Greenland ice-sheet contributions to the global sea level for the future-climate experiment under A1B scenario range from 5.4 to 38.7 cm at 500 years from the present-day. The projected ranges are larger for experiments where future-climate scenarios are amplified by a factor of 2, as 8.5 to 142.6 cm. It is one of the objectives of the SeaRISE project to show the possible range of uncertainties in the ice-sheet projection of current ice-sheet models, because no single model can be identified to be the best in every aspect (Bindschadler et al., 2013). The approach of the SeaRISE project is rather unrestricted: some aspects in the experiment protocol are standardized, while many others are left to the individual participants. The former includes part of boundary conditions of the ice-sheet model, such as the present-day surface temperature, surface accumulation and bedrock topography. Future scenarios are also provided. Scenarios for future surface climate changes, for example, hundred-year time series of surface temperature, precipitation, and surface melting are provided. The latter includes structural differences in ice-sheet models such as model numerics or approximation level, and the treatment of some boundary conditions such as the surface mass balance scheme.

Bindschadler et al. (2013) identify the differences in the methods to compute the surface mass balance among the participants as the primary source of the diversion in the results of future-climate experiments of the Greenland ice-sheet. Nowicki et al. (2013) further concluded that the variations in the initial ice volume, and thus the initialization of the ice-sheet topography, is another source of uncertainties. However, detailed quantitative evaluation of the reasons for the diversion were beyond the scope of the two papers.

The present paper performs a "one-model" approach to evaluate the relative impact of the various factors onto Greenland ice-sheet projections under the SeaRISE protocol. The numerical model used in this paper is IcIES (Ice-sheet model for Integrated Earth-system Studies), which also participated in the SeaRISE experiments. As sum-
5   marized in Table 2 in Bindschadler et al. (2013), there are at least ten characteristics with different implementations among the participating ice-sheet models of SeaRISE, most of which have two or more variations. Some concern numerical aspects, such as grid resolution and time-stepping, and others are physical aspects, such as ice flow mechanics and surface mass balance.
10   This paper does not intend to cover the sensitivities of all of the aspects. The initialization methods and the surface mass balance methods, proposed in Bindschadler et al. (2013) as possible sources of variation, and three more characteristics, the bedrock topography boundary condition, the basal sliding methods, and the treatment of advance/retreat in the ice-sheet margin, are chosen to investigate sensitivities in the
15   present paper. Of the four different sets of future scenarios under the SeaRISE protocol, the surface climate experiment (C1 to C3), the basal sliding experiment (S1 to S3), the ice-shelf melting experiment (M1 to M3), and a combination experiment, the present paper only revisits the surface climate experiment.
     In the next section, the five model set-up characteristics of focus in this study are
20   introduced to demonstrate the variety of choices among SeaRISE individual participants used in Bindschadler et al. (2013). In Sect. 3, a model description of IcIES is given to describe the set-up adopted in the submission of Bindschadler et al. (2013). In Sect. 4, we describe the set-up of the five characteristics to replace the IcIES standard configuration in the present experimental design. Results and discussion follow to
25   identify and compare the possible sources of spread among the results of the SeaRISE participants.

2 Candidates for sources of spread in SeaRISE projections

2.1 Bedrock topography

SeaRISE provides several different versions of the present Greenland ice-sheet topography (available at http://websrv.cs.umt.edu/isis/index.php/Present_Day_Greenland).
"Greenland Developmental Data Set" (hereafter referred to as *dev1.2*). This data set includes a Jakobshavn trough in the bedrock and bathymetry topography of Bamber et al. (2001) (the second last version in the protocol). For the latest protocol, the bedrock topography including a new compilation of the subglacial troughs over Jakobshavn Ibsrae, Helheim, Kangerlussuaq, and Petermann glaciers following Herzfeld et al. (2012) is proposed (hereafter refer to as *JHKP*). Although the differences between these datasets are local, significant differences in the simulated global features are possible. Herzfeld et al. (2012) present the significant difference on the present-day simulated topography and velocity field by using the JHKP dataset and an older data set without inclusion of the above four glacier troughs (corresponding to a version before dev1.2 in SeaRISE). In addition, significant differences are shown in the response of the Greenland ice-sheet to doubled-sliding experiments over 500 years, (i.e. equivalent to the S3 experiment in SeaRISE).

2.2 Basal sliding formulation

The available methods to compute basal sliding have some degrees of freedom. One method applies a Heaviside function at the pressure-melting point of the basal temperature, while others apply a smooth sliding transition around the pressure-melting point (Hindmarsh and Le Meur, 2001), partly for numerical stability and partly for physical reasons to introduce sub-grid scale variation of the basal sliding. Some models in SeaRISE explicitly document such smooth transition to implement melting at submelting point temperatures.

Title Page

Abstract	Introduction
Conclusions	References
Tables	Figures

|◄ | ►|

◄ | ►

Back | Close

Full Screen / Esc

Printer-friendly Version

Interactive Discussion

2.3 Initialization method

Obviously, the accuracy of the simulated present-day ice-sheet is crucial for future projections. It is possible that small errors in the simulated present-day state may affect the short-term projections (Arthern and Gudmundsson, 2010; Yan et al., 2013). In addition,
5 since the climate depends on the surface topography and ice extent, present-day climate forcing computed in the simulation may already have some bias. This bias occurs both for simulations with ice-sheet models coupled to sophisticated climate models, but also in simulations using simple climate parameterizations. Some previous studies compute surface temperature by a combination of a reference field obtained from
10 observation-based studies and their perturbation via the lapse-rate and changes in surface topography relative to the present-day observed surface topography. This implies that the computed surface temperature field in the model is identical to the observation only when the modeled surface topography is the same as the observation.

The choice of initialization method was left to participants in SeaRISE, and three dif-
15 ferent techniques were applied by the SeaRISE/Greenland participants. One method is called initialization by "tuning", which inverts given data fields, e.g. basal friction coefficients, to adjust present-day observation fields, e.g. surface velocity. Internal temperature fields are usually assumed to be in a steady-state with computed velocity fields under the present-day conditions. The second method is called initialization by "spinning-
20 up", whereby the model is run with the input of climate history of glacial/interglacial cycles, e.g. derived from the GRIP ice-core record. A variation of initialization by "spinning-up", hereafter referred to as "free spinning-up", allows the ice-sheet topography to evolve freely under a prescribed climate history. The other initialization method is referred to as "fixed topography spinning-up", where the ice-sheet topography is
25 fixed through the spin-up phase at a slightly smoothed measured present-day topography while ice-sheet temperatures freely evolve. The "fixed topography spinning-up" is a hybrid of the two techniques where the initial topography can be very close to the present-day observation while ice-sheet internal states include influence of the long-

term climate history. One major drawback is that the flow and temperature fields in the initial state are not in equilibrium (Goelzer et al., 2013), which leads to an artificial drift to restore the equilibrium after allowance of evolution in the topography.

A number of previous studies have focused on the initialization methods and their impact on the simulation of the Greenland ice-sheet. Rogozhina et al. (2011) compare the simulated present-day Greenland ice-sheet obtained by several initialization methods including free transient spinning-up. Goelzer et al. (2013) present a series of Greenland ice-sheet simulations with yet another hybrid technique to incorporate the influence of long-term climate history and obtain an initial ice-sheet topography close to the present-day conditions, by adjusting ice-temperature profiles and synthetic corrections over the surface mass balance. They conclude that the uncertainty arising from the surface mass balance methods and scenarios have larger impact on the sensitivity of short-term projection of the Greenland ice-sheet than those from the initialization methods, but the experimental settings were not the same as the SeaRISE experiment. Yan et al. (2013) compare the evolution of the Greenland ice-sheet to future-climate scenarios between two spin-up methods: free spinning-up under transient and steady-state climate forcing. Both the simulated present-day ice-sheet topography and the simulated surface mass balance are different, thus the impact of the difference in the initialization method includes all of these components. Seroussi et al. (2013) find that the ice-sheet model is far more sensitive to changes in external forcing than its initial temperature for a hundred-year scale experiment, while future scenario experiments from different initial conditions are not discussed. Aðalgeirsdóttir et al. (2014) present a series of Greenland ice-sheet simulations using free transient spinning-up as well as a *flux-corrected* initialization method, in which the surface mass-balance during the initialization is modified such that the simulated present-day topography is close to observation. They conclude that the initialization methods are an important source of uncertainty.

So far, influence of the "fixed topography spinning-up" has not been discussed, which is a main target of the present paper. In addition, although Nowicki et al. (2013) con-

Title Page

Abstract | Introduction

Conclusions | References

Tables | Figures

|◄ | ►|

◄ | ►

Back | Close

Full Screen / Esc

Printer-friendly Version

Interactive Discussion

clude that variation of the initial ice volume may be a source of the uncertainties in SeaRISE results, the influence of different choices for the initialization methods are not qualitatively evaluated. This paper extends their discussion and shows the relative significance to the short-term projection among other possible methods.

2.4 Treatment of advance of the ice-sheet margin

Precise simulation of the ice-sheet margins (ice-sheet extent) is a challenging issue. When ice-sheet topography and extent are allowed to evolve freely during the future-warming experiments, it is possible to show sudden jumps in the position of the ice-sheet margin over many regions. Such changes reflect a strong flux imbalance near the margin in the simulated present-day state. Some participants in SeaRISE artificially prohibit such cases either by fixing the position of the ice-sheet margin, or by limiting the advance of ice-sheet margin (i.e. retreat is allowed). This is just an assumption, and previous studies have not demonstrated its influence on the sensitivity of the results, and so this issue is explored here.

2.5 Surface mass balance

The four aspects described above involve the technical rather than physical configuration, thus replacement of these four methods may describe the impact of indirect processes in the model to climate warming. The method to compute the surface mass balance to drive ice-sheet models instead affects the physical configuration and uncertainty relating to this aspect describes the direct impact of the model to response of Greenland ice-sheet to climate warming. There have been a wide range of methods used to compute surface melting and/or surface mass balance in previous works including SeaRISE.

The method to compute surface mass balance was left to individual choice in the SeaRISE project, which provided the future scenarios of precipitation, surface temperature, and surface melting, but whether or not to adopt unique parameterization of

surface melting using the scenarios of precipitation and surface temperature was left to individual models.

Most participants adopt a form of the "positive degree-day" (PDD) scheme Reeh (1991) to compute surface melting. Even models using the PDD scheme, however, can vary in one or more parameters used in the scheme, e.g. the conversion coefficients from simulated degree-day to melting, the SD of short-term statistical air temperature fluctuation, and so on. Some previous studies present how variation in PDD schemes and their coefficients can influence present-day and future simulation of Greenland ice-sheet (e.g. Stone et al., 2010). Bindschadler et al. (2013) argue that the variation of the surface mass balance method is the likely primary source of the diversion in the results of future-climate experiments, although this assertion has not been qualitatively evaluated. This paper will demonstrate the relative significance of the surface mass balance method on the short-term projection compared to other model settings.

3 Model description

The time-dependent, three-dimensional and thermodynamically coupled model used in this paper as well as in the SeaRISE project, called IcIES (Ice-sheet model for Integrated Earth-system Studies), is described in Saito and Abe-Ouchi (2005), Greve et al. (2011) and Bindschadler et al. (2013). The model computes the evolution of the ice thickness, bedrock elevation and ice temperatures under a history of climate forcing, given in terms of surface mass balance and surface temperatures, which may depend on the computed ice-sheet topography. The model parameters are the same as those described in Greve et al. (2011). In the present paper, the model domain spans $1500\,\text{km} \times 2800\,\text{km}$, with ($151 \times 281$ grid-points) corresponding to a horizontal resolution $10\,\text{km}$.

The evolution of surface elevation is determined by the continuity equation for the local ice thickness with a history of surface mass balance field. The temperature distribution is calculated with the thermodynamic equation with the surface temperature

and geothermal heat flux given at the surface and base, respectively. Changes in the bedrock elevation are calculated by a linear model expressing local isostatic rebound with a prescribed time constant.

The shallow ice approximation is applied (Hutter, 1983) using Glen's flow law with an exponent of $n = 3$ (Paterson, 1994) for the velocity computation. The horizontal velocity vector $\boldsymbol{v}_H$ is calculated for the given surface elevation h and bedrock topography b,

$$\boldsymbol{v}_H = \boldsymbol{v}_B - 2(\rho_l g)^n \left[\left(\frac{\partial h}{\partial x} \right)^2 + \left(\frac{\partial h}{\partial y} \right)^2 \right]^{\frac{n-1}{2}} \int_b^z dz'\, E\, A(T)(h - z')^n \times \nabla_H h, \tag{1}$$

where g is acceleration of gravity, ρ_l is the density of ice, and $\boldsymbol{v}_B$ basal sliding velocity, respectively. The rate factor $A(T)$, through which the velocity and temperature fields are coupled, follows Paterson (1994) and Huybrechts (1992). The formulation in Paterson (1994) is different from the one in Cuffey and Paterson (2010). We use the former in this study for a historical reason, to keep it consistent with the past numerical studies using IcIES including the submission to SeaRISE. Another reason is that the focus of this paper is on sentisitivies to different external and technical configurations, but not on "ice-flow" physics. The enhancement factor E in Eq. (1), which controls the softness of ice implicitly reflects the effect of impurity and/or anisotropy of ice. It is used as a tuning parameter to improve the agreement between measured and modeled surface topography. In the present paper uniform value $E = 3$ is adopted in all experiments.

The basal sliding velocity $\boldsymbol{v}_B$ is computed with the Weertman sliding law, with an allowance for sub-melt sliding following Hindmarsh and Le Meur (2001),

$$\boldsymbol{v}_B = -C_B \frac{\tau_B{}^p}{N_B{}^q} \times f(T_B') \,, \tag{2}$$

where τ_B, N_B, T_B' are basal shear stress, basal normal stress, and basal temperature relative to the pressure-melting point, respectively. The function $f(T_B')$ controls the occurrence of basal sliding (see Sect. 4). Following Huybrechts and de Wolde (1999),

the exponents p, q and the coefficients C_B are set as 3, 1 and $1.8 \times 10^{-10}\,\mathrm{N^{-3}\,yr^{-1}\,m^8}$, respectively, for the standard configuration (`v1`, see Sect. 4).

The computation of the annual and summer mean surface temperatures follows Fausto et al. (2009), which depends on the surface elevation, longitude, latitude and the background temperature field. Monthly mean temperatures are obtained by interpolation of the annual and summer mean fields using a sinusoidal function. The surface mass balance field is computed as the sum of the accumulation and ablation fields. The present-day mean annual precipitation (Ettema et al., 2009) is modified by a temperature dependent function following Huybrechts et al. (2002). Conversion from the precipitation to the accumulation rate is computed statistically as in Huybrechts and de Wolde (1999), which is a function of the mean monthly temperature. Ablation (surface melting) is computed using the Positive Degree-Day (PDD) method of Reeh (1991), which relates ablation to both air temperature and snow accumulation. The amount of melting is computed as the product of number of positive degree days and PDD factors obtained by observations. It considers the possibility for melting even when the average daily temperature is below the freezing point and different melt rates for melt of snow and ice due to the albedo difference (Braithwaite and Olesen, 1989), and the production of superimposed ice and warming caused by the phase change. This method is adopted in most numerical studies with ice-sheet models (Ritz et al., 1997; Greve, 2000; Huybrechts et al., 2002). Four parameters control the surface melting in the PDD scheme in IcIES, the PDD factor for ice melt, β_{ice}, PDD factor for snow melt, β_{snow}, the SD of short-term air temperature fluctuation, σ, and the saturation factor for the formation of superimposed ice, P_{max}. The selection of the values of these parameters are described later.

All experiments in the present paper are performed with the newer revision of IcIES than that used for the SeaRISE project. To obtain stable simulations over all the experiments with a unique method, some modifications of the numerical representation were implemented. The physics and the mathematical formulation of the physics were not changed. The difference in the volumes of the simulated Greenland ice-sheet for identi-

cal configurations varied at most by 0.3 %, which does not affect the conclusions of the present paper. Therefore, although the model itself is slightly modified, the experiment design used for the submission is hereafter referred to as "IcIES" original configuration.

4 Experimental design

Four different future-climate experiments are presented in Bindschadler et al. (2013): the surface climate experiment, the basal sliding experiment, the ice-shelf melting experiment and a combination experiment. The present paper focuses on the surface climate experiment, while the other three experiments are left for future studies. The surface climate experiment leads to less abrupt changes after the perturbation is applied than the other three, which is expected to emphasize the differences among various modelling approaches. In this future-climate experiment, changes in the climate conditions on the upper surface of the ice-sheet are prescribed. Future scenarios of two fields, surface temperature and precipitation, are provided. The scenarios were calculated from the results of A1B scenario experiments by 18 climate models which participated in the Fourth Assessment Report, compiled by Bindschadler et al. (2013). A "A1B climate change" scenario, C1, over 500 year is now available, where the first 100 years are obtained from climate model results, and the climate state of the final 400 years is kept constant at the year 100 climate. Two more "enhanced climate change" scenarios, C2 and C3, are defined where the climate change of C1 with respect to the present day is amplified by factors of 1.5 and 2.0, respectively. In addition, a "constant present day climate" scenario, C0, is defined for reference experiments.

One of the major uncertainties relating to ice-sheet dynamics stems from the basal sliding processes because they are poorly understood due to the difficulties in direct observation (e.g. Nowicki et al., 2013). Often, the parameters relating to basal sliding are tuned to match present-day observed features such as ice-sheet topography and/or the surface velocity. Some models adopt spatially homogeneous parameters (e.g. Robinson et al., 2011), while others apply an inversion technique to compute spa-

tially variable parameters (e.g. Seroussi et al., 2013). Although it is important, such fine tuning is beyond the scope of the present paper. Rather, the impact of homogeneous changes in the basal sliding coefficients are presented to interpret the results of the present paper. Generally, the simulated ice-sheet thickness is too large, especially near the margin (Nowicki et al., 2013), which requires larger basal sliding coefficients to reduce the error. In this paper, the cases of uniform doubled ($\mathtt{v2}$) and quadrupled ($\mathtt{v4}$) basal sliding coefficients are examined. All of the experiments are repeated using these coefficients throughout the simulation. It is worth mentioning that the enhanced sliding experiments in the present paper differ from the "Basal-sliding experiment" (e.g. S1) presented in SeaRISE. The former keeps the same value for the sliding coefficients over both the spin-up and the future, while the latter changes the coefficients for the future experiment.

Table 1 summarizes the sensitivity experiments in the present paper. The original IcIES submission, which is referred to as configuration $\mathtt{O}$, adopts the following methods for the five characteristics:

– "Greenland Developmental Data Set" (dev1.2) for the bedrock topography;

– basal sliding follow the Weertman law without allowance of submelt sliding;

– "free" spinning-up method to initialize the present-day ice-sheet topography;

– "free" advance/retreat of ice-sheet margin in response to the climate boundary condition;

– positive degree-day method for surface melting following Tarasov and Peltier (2002) for the choice of PDD factors.

A series of four experiments, $\mathtt{A}$-$\mathtt{B}$-$\mathtt{D}$-$\mathtt{E}$, is the sequence of one-by-one replacement in four methods: bedrock, submelt sliding, initialization and margin advance, starting from the original configuration $\mathtt{O}$. Three configurations $\mathtt{B}'$, $\mathtt{D}'$ and $\mathtt{E}'$ were performed with an additional replacement in the surface mass balance computation. The details of these replacements are described below.

Title Page

Abstract | Introduction

Conclusions | References

Tables | Figures

◄ | ►►

◄ | ►

Back | Close

Full Screen / Esc

Printer-friendly Version

Interactive Discussion

4.1 Bedrock topography (A)

The bedrock topography dev1.2 used in the original configuration O is replaced by the JHKP data set in experiment A. All the procedures are then repeated with the new bedrock data.

4.2 Basal sliding formulation (B)

The original IcIES submission adopts a Heaviside function at the pressure-melting point for the occurrence of basal sliding. It corresponds to the use of a binary operator with $f = 1$ if the bottom temperature is at the pressure-melting point and $f = 0$ otherwise, see Eq. (2). The Heaviside-function switch in A is replaced by an exponential function of the basal temperature following Greve (2005) and Greve et al. (2011),

$$f(T'_B) = \exp\left[T'_B/\gamma\right] \ , \tag{3}$$

where the parameter $\gamma = 1$ is in the present paper.

4.3 Initialization method (D and D_s)

For the original submission, IcIES used the "free spinning-up" method. The background temperature history is based on the oxygen isotope record of the GRIP ice-core (Dansgaard et al., 1993; Johnsen et al., 1997), which is provided by SeaRISE as a time series of temperature from 125 ka to the present. At the beginning, a steady-state simulation is performed under the climate field at 125 ka, and from this steady-state condition, the ice thickness and temperature and the bedrock topography are allowed to evolve freely until 0 ka.

Two other methods are tested in the present paper: the "fixed topography *transient* spinning-up" and the "fixed topography *steady-state* spinning-up". In the first method, similar to the free spinning-up, a steady-state simulation is performed under the climate field at 125 ka with fixed ice-sheet and bedrock topography of the present-day state and

Discussion Paper | Discussion Paper | Discussion Paper | Discussion Paper |

Title Page

Abstract | Introduction

Conclusions | References

Tables | Figures

|◄ | ►|

◄ | ►

Back | Close

Full Screen / Esc

Printer-friendly Version

Interactive Discussion

only the temperature can evolve. Subsequently, the climate history from 125 to 0 ka is used to force the internal ice-sheet temperature. Thus the ice-sheet topography used as the initial condition for the future-climate experiment is identical to the present-day condition. Smoothing of the ice-sheet topography as some SeaRISE participants is not applied for the present paper, in order to obtain the identical topography among runs with different model parameters. Experiment D uses the same configuration as B except for using this fixed topography *transient* spinning-up.

In the "fixed topography *steady-state* spinning-up" method, a steady-state simulation is performed under present-day climate and topography fields with evolving temperature. This initialization method mimics the "tuning" method, where the ice-sheet topography is very close to present-day observations, while the influence of the long-term climate history is excluded. This initialization requires an inversion of, e.g. the coefficients of basal velocity, which is not implemented in IcIES, but is mimicked by different basal sliding enhancement factors. Experiment D_s uses the same configuration as B except for using the above fixed topography *steady-state* spinning-up.

4.4 Treatment of advance of the ice-sheet margin (E)

Both advance and retreat of the ice-sheet margin are freely allowed in the original configuration of IcIES. The configuration E is equivalent to D except that only retreat in the ice-sheet margin is allowed after the present-day simulation. The initialization phase of configuration E is identical to that of D, but the advance in the ice-sheet margin is not allowed under future-climate runs.

4.5 Surface mass balance (B′ etc)

In the original IcIES submission, the PDD factor for ice melt is a cubic function of the local mean July surface temperature with a range between a minimum of 8.3 mm and a maximum of 17.22 mm ice equivalent per day per degree (Tarasov and Peltier, 2002). The factor for snow melt is a linear function of local mean July surface temperature with

the range between a minimum of 2.65 mm and a maximum of 4.3 mm ice equivalent per day per degree. The SD of the short-term statistical air temperature fluctuations to compute daily temperatures from monthly temperatures is set as 5.5 K in the IcIES original submission, which is slightly larger than the value of 5.2 K in Tarasov and Peltier (2002).

Some models adopt constant (temperature-independent) coefficients, such as 3 and 8 mm ice equivalent per day per degree for snow and ice, respectively, and a SD of air temperature variations of 5.5 K, following Huybrechts and de Wolde (1999). In the present paper, this combination of the PDD parameters is tested to evaluate the impact of the difference in the surface melting methods and especially to compare the relative sensitivity to the four other more technical aspects.

4.6 Impact of "fixed-topography" transient spin-up

One aspect remaining to be discussed is the impact of non-equilibrium internal states originating from the "fixed-topography" transient spin-up. Since there is a feedback between climate and ice-sheet topography, the difference between "free spin-up" and "fixed topography spin-up" includes both the effect of internal temperature and also the effect of the initial topography. One way to minimize the initial discrepancy and to separate the impact of non-equilibrium internal states is to perform a "free spinning-up" simulation that ends with the same topography at the present-day. The impact of the internal non-equilibrium state is evaluated as follows: The final state of the spin-up phase of experiment B (or B') is adopted for the "fixed-topography" transient spin-up, which is referred to as experiment F (or F'). Thus the difference between experiments B (B') and F (F') only stems from the internal thermal state due to the initialization methods, both having identical initial topography.

To evaluate the impact of "no memory" of the transient past climate, "fixed-topography" *steady-state* spin-up experiments are performed (experiment D_s, D'_s, F_s and F'_s). For the configuration of D_s and D'_s, the topography is fixed at the present-day observation and internal temperature distribution is computed until reaching a steady-

state under the present-day climate field. For the configuration of F_s and F'_s, the topography is fixed at the final topography of the spin-up phases of experiments B and B', respectively.

5   Results

Table 2 summarizes the simulated ice-sheet volumes at the end of the initialization phase (or at the beginning of future-climate scenario experiments) compared to the present-day observations. Under configuration O, the overestimation of the ice-sheet volume is within +6 % and with increased basal sliding coefficient v4 within 0.5 % of the present-day observations. The good match of the simulated volumes can be explained by an overestimation around the margin and an underestimation over the interior regions (e.g. Bindschadler et al., 2013; Yan et al., 2013).

Bindschadler et al. (2013) present their results in terms of the simulated time series of volume above flotation (VAF) under future climate warming scenarios, C1,C2 and C3, relative to that under the constant climate scenario C0. Figure 1 shows the results of the present paper following the SeaRISE analysis under future-climate scenarios C1 with a standard basal sliding coefficient v1. Figure 1 also shows the ranges of the results of the eight SeaRISE participants at 100, 200, 500 years from the present, given in Table 3 of Bindschadler et al. (2013). The result of configuration O, which is a simulation corresponding to the original IcIES submission, show the largest response among the experiments.

Figures 2 and 3 show simulated changes of VAF at 500 years obtained by all experiments in the present paper under the future-climate scenarios C1, C2 and C3 for the standard (v1), doubled (v2), and quadrupled basal sliding coefficients (v4).

The results of configuration O, show volume losses of 34.1, 72.1 and 142.8 cm sea level equivalent at the time 500 year under climate scenarios C1, C2 and C3, respectively. Standard basal sliding cases v1 under all future climate scenarios are within the range of original SeaRISE results. Simulated responses become larger with enhanced

basal sliding coefficient, and some cases are still within the original range of results, while some are above the range, for example, the simulated VAF response of `C3:v4` is +17 cm.

5.1 Bedrock topography

Configuration `A` is equivalent to `O`, except that the bedrock topography dev1.2 is replaced by the JHKP topography. Simulated VAF responses are already affected by replacing the bed topography of a few regions, however, are less than +2.2 cm under all the combinations of climate and sliding coefficients (Fig. 2).

5.2 Basal sliding formulation

Configuration `B` is equivalent to `A` except for the inclusion of sub-melt sliding during both the initialization and future scenario phases. Table 2 shows the simulated volumes at the end of the initialization with configuration `B`. The introduction of the sub-melt sliding results in a wider sliding area and therefore in a smaller ice-sheet volume due to enhanced outward ice flow. The standard basal sliding coefficient case `v1` shows ice-sheet volumes close to present-day observations (1.7 % overestimation). Similar to other configurations, such as `O` and `A`, the increase of the basal sliding coefficient leads to smaller present-day ice-sheet volumes. In the case `v4` with four-times coefficients, the resulting present day ice volume underestimates observations by more than 10 %. Under configurations `O` and `A`, the spread of present-day ice-sheet volumes are around 5 % of the observed value among three basal sliding coefficients cases, and lies more than 12 % under `B`.

Figure 4a–c shows simulated present-day ice-sheet topography obtained by `B:v1` to `B:v4` cases, respectively. The interior part of the ice-sheet becomes lower with an increasing basal sliding coefficient. In addition, the ice-covered area around the north-west region is much reduced with a higher basal sliding coefficient in particular on `B:v4` case, which partly contributes to the overall underestimation in volume.

Title Page

Abstract | Introduction

Conclusions | References

Tables | Figures

◄ | ►

Back | Close

Full Screen / Esc

Printer-friendly Version

Interactive Discussion

The replacement of submelt sliding treatment affects the VAF response greater for higher climate scenarios and larger sliding coefficients as shown in Fig. 2. The `C1:v1` case results in a loss of 36.5 cm at 500 year, (which is about 1 cm more than in case `A`. The largest difference in the ΔVAF is +26.4 cm for the `C2:v4` case.

5.3 Initialization method

Configuration `D` is equivalent to `B` except that the ice-sheet initial condition is obtained by a fixed topography spinning-up given by the present-day observation. The simulated response of the VAF is 26.0 cm for `D` under the `C1:v1` case, therefore it has −10.5 cm impact relative to `B`. This is large enough to cancel the impacts of the treatment bedrock topography and submelt sliding (Fig. 2). Under the `C2` and `C3` cases, ΔVAF are 52.6 and 111.6 cm, which shows −24.5 and −39.3 cm impact, respectively. Thus, the impact of the replacement of the initialization method reaches around 1/3 of the range of the original SeaRISE experiments. Even under larger basal sliding coefficients, cases `v2` and `v4`, ΔVAF are significantly reduced due to the different initialization methods, which are large enough to cancel the effect of including submelt sliding.

Figure 3 shows the changes in VAF relative to the corresponding initial condition obtained by experiments `B`, `F` and `D`, over all the combinations of climate scenarios and sliding coefficients, including the corresponding constant future-climate scenario case `C0`.

Configuration `F` is equivalent to `B` except that the ice-sheet initial condition is obtained by a fixed topography spinning-up as the final state of configuration `B`, which means that the initial topography for future-climate runs are identical. Since internal thermal states are not in equilibrium under configuration `F` due to the artificial prohibition of topography evolution, the thermal conditions drift to restore the equilibrium during the future climate run even under the constant climate simulation. Of all the combinations examined in the present paper, the differences in the final states of ΔVAF between `B` and `F` are smaller than the differences in ΔVAF between `B` and `D`. This means that the model sensitivity of the internal non-equilibrium thermal states is smaller than the sensitivity to the the

initialization method options, when they evaluated in terms of changes relative to the constant climate experiment. Through the elevation-ablation feedback, the impact of the non-equilibrium thermal state is larger in cases of higher sensitivity. The maximum impact in the present paper is +14.5 cm sea level equivalent for `F` under the `C3:v4`
5   case, which is 10.5 % of the variability of corresponding `D` cases.

Configuration `F_s` is equivalent to `F` and `B` except that the initial condition of the ice-sheet is obtained by a fixed topography "steady-state" spinning-up as the final state of configuration `B`. All the experiments show almost identical sensitivity of VAF between steady-state and transient spin-up, in terms of relative changes in VAF to
10   the corresponding constant climate scenario cases. Seemingly, if an initial state with free spinning-up methods ends at the observed topography, the time evolution of VAF comes close to the one obtained by fixed spinning-up methods, both under transient climate scenarios and under the constant present-day climate scenario imposed for the first 500 years.

15   **5.4   Treatment of advance of the ice-sheet margin**

The initialization phase of configuration `E` is identical to that of `D`, but advance of the ice-sheet margin is not allowed while the retreat is freely allowed under future-climate runs. Prohibiting of ice-margin advance has a smaller impact than the choice of initialization methods (Fig. 2). The simulated response of VAF is 19.8 cm in experiment `E`, −6.2 cm
20   relative to `D` under the `C1:v1` case. Thus, under mild climate warming scenarios like `C1`, the choice of initialization method and the margin treatment has dominant effect on the response of Greenland ice-sheet over 500 years. The impact of the replacement of the treatment of the margin is affected little by the choice of basal coefficients.

5.5   Surface mass balance

25   Figure 2 shows the simulated changes in VAF under all of the combinations of climate scenarios and basal sliding coefficients by the series of experiment B', D' and E'.

Surface mass balance is replaced from B to B′, and after that, the same replacement sequences are followed as B to E (initialization and margin treatment).

Configuration B′ is equivalent to B, except that the surface melting parameterization of Tarasov and Peltier (2002), which was used in the IcIES original submission, is replaced by Huybrechts and de Wolde (1999), which was used by some of the SeaRISE participants. The future-climate runs C1 and C0 and the initializations are repeated using the new PDD methods. Table 2 shows the simulated initial volumes under the configuration of the B′ series and Fig. 2 shows the simulated changes in VAF under all of the combination of climate scenarios and basal sliding coefficients by the series of experiment B′, D′ and E′.

With the change of the surface mass balance method, the simulated present-day ice-sheet volumes become larger by about 4 %. Figure 4d–f shows simulated present-day ice-sheet topographies obtained by experiments B′:v1 to B′:v4, respectively. The main difference between B and B′ is found in north-western Greenland. The retreat of the ice-sheet margin over north-western Greenland is not seen in the B′:v4 cases (Fig. 4f). Changes over the interior region (around the summit) are small because the change in method influences primarily the ablation area near the ice-sheet margin.

Figure 2 shows a volume loss of 28.2 cm sea level equivalent at 500 year for configuration B′, thus replacing the PDD methods in the C1:v1 case has an impact of ∼ −8.3 cm This impact is slightly smaller than the impact of −10.5 cm by replacing the initialization methods from B to D. The smaller sensitivity partly stems from the over-estimation in the present-day topography. Since the simulated initial volume is larger, less surface melting is expected because of the elevation-temperature feedback. Under stronger warming scenarios, the impact of the replacement of the surface melting method from B to B′ is similar or even larger than that of the initialization method from B to D, which are −21.9 and −50.8 cm under C2 and C3, respectively. Similar to the replacement of initialization methods, the large impact due to different basal-sliding formulation is canceled by the replacement of the surface melting method and the results become closer among three cases of basal-sliding coefficients under the same climate

scenarios. Through all combinations of climate scenarios and basal sliding coefficients, a significant influence in the simulated responses of VAF due to the different surface mass balance methods are shown. As shown in Fig. 2, the difference in the surface melting methods has dominant and similar influences on simulated responses as the initialization methods.

Similarly, configurations D′ and E′ are equivalent to D, and E, respectively, except for the surface melting parameterization. Under the lower future climate scenario C1 (Fig. 2a), the influence of the replacement of surface mass parameterization is comparable to that of replacement of both the initialization method or the treatment of ice-sheet margin (B′ vs. D; D′ vs. E). Under the higher future-scenario C3, the influence of the former becomes even larger than those of the latter. Simulated responses in VAF are reduced to around 60 % of those obtained using the original surface mass balance parameterization (B vs. B′; D vs. D′; E vs. E′) under C3 future-climate scenario.

Configurations F′ and F′$_s$ (Fig. 3), are identical to B′ except that the initial condition of the ice-sheet runs are obtained by a fixed topography "transient" and "steady-state" spinning-up, respectively. In both experiments, the ice-sheet topography is fixed at the final state of configuration B′. Similar results are obtained with both surface mass balance parameterizations. Of all of the combinations in the present paper, the differences in the final states of ΔVAF between B′ and F′ are smaller than the differences between B′ and D′. This means that the impact of the internal non-equilibrium thermal state is smaller than the sensitivity to the initialization methods, with respect to the constant climate experiment. In addition, the influence of non-equilibrium thermal states on the VAF is smaller for both steady-state and transient spin-up.

The influence of the internal inconsistency and of surface mass balance parameterizations can be compared through the results of F and B′. Comparison between the results of F (B plus different initialization) and B′ (B plus different surface mass balance) show the relative influence of the internal inconsistency and the surface mass balance parameterization. Further, of all the combinations considered in the present paper, the impact of the internal non-equilibrium thermal state to the simulated sensitivity of VAF

is smaller than the impact of the difference in the surface melting methods for both a steady-state and transient spin up.

6 Discussion

The four methods examined in the series of experiment O-A-B-D-E (bluish group in Fig. 2) are related to technical aspects of the ice flow but do not relate to the climate scenarios. Among these four aspects, the inclusion of submelt sliding enhances the ice-sheet response strongest (A to B), but using "fixed-topography" spin-up cancels and even reduces this impact (B to D). Prohibition of ice-sheet advance is a secondary influence that can reduce the sensitivity (D to E). The results show generally that as simulated response in VAF is reduced, the spread of the results due to different basal sliding coefficients becomes small. For the lower future-climate scenario case C1, the combination of all four aspects (Fig. 2a) affects the volume loss as much as 42 %, which leads to the response of 19.8 cm sea level equivalent in experiment E. This value is very close to the average of SeaRISE participants (19.2 cm sea level equivalent) presented in Bindschadler et al. (2013), regardless of the basal sliding coefficients. For higher future-climate scenario case C3 (Fig. 2c), the combination of all four aspects affects the volume loss by as much as 30 % of the total response, which is not enough to explain the large deviation of O from the average. The spread of the results due to different basal sliding coefficients is slightly larger under the C3 scenario. Thus the source of spread in SeaRISE experiments can only partly be explained by variations in the experimental configuration of technical aspects, but mostly by the initialization method and slightly less by the treatment of the ice-sheet margin evolution.

The uncertainty in the methods to compute surface melting can further influence the model sensitivity. Configuration E′ replaces all four technical aspects as well as the surface mass balance compared to the original configuration O. E′ results in a volume loss which is smaller than the average of the SeaRISE experiments for C1 future-climate scenario. Even for the highest climate scenario, case C3, the volume response

is slightly smaller than or close to the average of the SeaRISE experiments, regardless of the basal sliding coefficient (Fig. 2c).

As shown in the series of the experiments in the present paper, neither the method to compute the surface mass balance, nor the way to initialize the ice-sheet is identified as the primary source of the spread in SeaRISE experiments, as already discussed in Bindschadler et al. (2013) and Nowicki et al. (2013). The variation of the surface mass balance alone (B to B$'$) may have a certain influence on the ice-sheet sensitivity, however not enough to completely cancel the large volume response obtained by the IcIES original configuration (i.e. configuration O with v1 basal sliding). The influence of the initialization methods on the short-term ice-sheet sensitivity is comparable to the influence of uncertainties in the surface mass balance methods. Moreover, the influence of the artificial prohibition of the advance of ice-sheet margin is found to be secondary to the main two aspects but not negligible.

One drawback when using initialization methods, except for the "free" spin-up, is an artificial drift due to simulated temperature fields. The "fixed-topography" spin-up leads to non-equilibrium internal states, but the influence of this inconsistency is difficult to evaluate. Since there is a feedback between climate and ice-sheet topography, the difference between "free spin-up" and "fixed topography spin-up" cases includes not only the internal temperature effect but the effect of the initial topography and thus the surface mass balance at the beginning. The influence of internal non-equilibrium thermal states can be estimated indirectly by comparison the results between B and F or B$'$ and F$'$, where the corresponding two have identical topography but different internal states. Of all the combinations in the present paper, differences in the final states of ΔVAF between B and F or B$'$ and F$'$ are smaller than the differences in those between B and D or B$'$ and D$'$, respectively. This implies that, at least in terms of changes relative to the constant climate experiment, the influence of the internal non-equilibrium thermal states to the ice-sheet sensitivity is smaller than the influence of different initial states. The largest difference between B and F is found under the C3:v4 case, which shows a difference of +14.5 cm sea level equivalent between the two different internal non-

equilibrium thermal states. Since an expected counterpart of the D case, which has the identical topography to the present-day observation without artificial drifts, cannot be easily performed, an indirect evaluation is conducted as follows. If this effect is also holds for the D case, 10.5 % of the total sensitivity of the case is estimated to be due to the internal non-equilibrium state. Therefore, future-climate experiments initialized by fixed-topography spin-up are considered the preferable approaches for characteristic projections of the ice-sheet evolution by an ice-sheet model. In addition, in terms of changes relative to the constant climate experiment, steady-state and transient spin-up initializations show almost identical sensitivities during 500 year model runs.

Table 3 summarizes simulated changes in VAF of configurations B, F, D, and D$'$ relative to the corresponding constant future-scenario experiments Except for the lower sensitivity cases such as C1:v1 and C1:v2, the table shows that the effect of internal non-equilibrium states (B vs. F) is rather small compared to the effect of difference in surface mass balance methods (D vs. D$'$). Thus, the uncertainties due to surface mass balance must be the primary source of uncertainties in the simulated short-term future projections of the Greenland ice-sheet, rather than those due to ice flow characteristics.

Therefore, although it cannot be confirmed, if a *perfect* spin-up (free evolution spin-up under transient climate ending with the present-day observed topography) could be obtained, then it can be expected that the VAF response of such an experiment would be close to that obtained using a fixed-topography spin-up with the present-day topography, and also it may be better than using a free spin-up under the same configuration. Thus, a future-climate experiment initialized by fixed-topography spin-up (with the present-day topography) can be considered a suitable approach for characteristic projection by an ice-sheet model. While not able to be fully confirmed, the analysis of the series of the experiment in the present paper suggests that the large sensitivity of IcIES can be attributed to the difference in the application of the technical methods such as initialization and free evolving margin, and the difference in the surface melting parameterization.

All the analysis in the present paper is examined using anomaly relative to the result of the "constant" future climate experiment C0 ("experiment minus control"), following the discussion of the SeaRISE methods (Bindschadler et al., 2013; Nowicki et al., 2013). In other words, trends in the evolution of the ice-sheet volume at the present-day, whether they are artificial or not, are excluded from the discussion. In reality, the trends arise as the result of long-term climate history. Since the trend is not necessarily zero, the actual future projection of the Greenland ice-sheet should be evaluated as the sum of the trend and the anomalies. The present paper concludes that such long-term memory has a smaller impact for the future *changes* in ice-sheet volume at least during next 500 years, compared with the changes due to future surface climate scenarios. Only a part of the surface climate experiments in SeaRISE has been revisited in the present paper. The same procedures applied here can be followed for other series of experiments (e.g. basal-sliding experiments), which are left for the next study.

7 Conclusion and prospects

The present paper revisits the future surface-climate experiments of the Greenland ice-sheet proposed by the multi-model intercomparison SeaRISE (Bindschadler et al., 2013). A series of sensitivity experiments has been performed, using the ice-sheet model IcIES, to identify sources of the spread in the SeaRISE multi-model intercomparison. Five aspects: surface balance parameterization, sliding, margin migration, initialization and bed topography, are chosen to replace the standard formulation of IcIES by those adopted in other models, and all the experiments are conducted from spin-up to the simulation of future evolution. The results show that the main sources of the spread in the SeaRISE experiments are the difference in the initialization methods and the difference in the surface mass balance methods. As already proposed in the SeaRISE papers, and confirmed quantitatively in the present paper, the impacts of these two aspects are of comparable magnitude. In addition, the treatment of ice-sheet margin migration in the simulations also has a non-negligible impact on the spreads among the

Title Page

Abstract   Introduction

Conclusions   References

Tables   Figures

Back   Close

Full Screen / Esc

Printer-friendly Version

Interactive Discussion

multi-model projections. Performance of an initialization technique with fixed ice-sheet topography through time while temperature is allowed to be evolved according to the surface temperature history is indirectly evaluated and found to provide an acceptable initial condition, at least for short-term projections.

5   The SeaRISE project, in which several ice-sheet models of different complexity participated to perform similar experiments, showed the divergence or convergence of current ice-sheet modeling. Furthermore, Nowicki et al. (2013) show detail and careful analysis of all the results both globally and regionally, to present how and where the models are consistent or inconsistent. However, the SeaRISE protocol is not strictly

10   controlled and most experimental configurations are left as the choice of the participants. Therefore, it is difficult to separate the effects of different choices by comparing only the submitted results. The present paper demonstrates that various implementations adopted in individual models can affect the simulated responses and how much they may contribute to the diversity in SeaRISE results. A one-model study, such as the

15   present paper, cannot cover all possible variations among the existing models. It would be preferable that all participating models perform one common and highly controlled experiment which allows effective identification of the uncertainties due to specific variations in ice-sheet models. The intercomparison experiments of the ice2sea projects (e.g. Edwards et al., 2014) mainly focus on model differences, and therefore provide

20   such controlled protocols but for the initialisation methods.

Here we propose a model intercomparison study to evaluate the uncertainties in modeled response that originate from modeled ice flow characteristics such as ice flow approximation level, basal sliding formulation and model resolution. The proposed experiment set-up, which is referred to as the "benchmark" experiment, consists of

25   a carefully controlled protocol to define the following characteristics:

- – Initialization of the present-day condition using either

    - – assimilation
    - – "fixed-topography" spin-up.

- Prepare "identical" climate forcing, that is not temperature but the spatial/temporal scenario of the surface mass balance with no topography or albedo feedback.

- Perform two short-term future-climate experiments, a constant climate experiment and a warming climate experiment.

5 - Advance of the ice-sheet margin must be limited to the present-day (initial) margin.

A demonstration of this type of experiment is presented in Appendix A. Since spinning-up methods are less controlled except for the ice-sheet topography, most types of ice-sheet models can easily perform this experiment, including very heavy full-stokes models, models using inversion techniques, and models using free evolu-
10 tion spinning-up over a long climate history. This experiment configuration is a compromise to allow choice of initialization method by individual model, but is, however, still proscribed enough to separate uncertainties and/or some feedbacks.

Appendix A: Demonstration of "benchmark" experiment

For a demonstration of the suggested benchmark experiment, configuration E_s'' is per-
15 formed by IcIES, which is the same as E_s and E_s' except for the future surface mass balance scenarios. Steady-state initialization under fixed present-day topography is performed, and the future surface mass balance is imposed using the SeaRISE datasets without any correction.

Actually, one participant, ISSM, in SeaRISE has similar configuration to the bench-
20 mark: initialization is based on inversion which enables initialization with a topography close to that of the present-day; surface mass balance is imposed on the SeaRISE datasets without any correction; and a fixed calving front is enforced. The simulated response of VAF for this experiment is 5.4 cm sea-level equivalent at 500 years from the present under C1 scenario, which is actually the minimum response among the
25 SeaRISE participants.

Figure A1 shows the simulated time series of VAF under `C1` scenario with three different basal sliding parameters `v1` to `v4`. The losses in VAF by IcIES are -10.8, -12.0, and -13.0 cm sea-level equivalent at 500 years with basal sliding configuration of `v1`, `v2` and `v4`, respectively, thus only 2.2 cm spread are due to the different basal sliding coefficient. The smallest responses in the present paper are obtained under E_s'' configuration, which is even smaller than configuration E' cases but still twice as large as the smallest result of SeaRISE participants (ISSM, upper end of the gray bar in Fig. A1). The difference of 5 cm sea level equivalent entirely stems from the difference in ice-flow characteristics between the two models, higher-order physics, anisotropic mesh, and inhomogeneous basal sliding coefficients.

References

Aðalgeirsdóttir, G., Aschwanden, A., Khroulev, C., Boberg, F., Mottram, R., Lucas-Picher, P., and Christensen, J.: Role of model initialization for projections of 21st-century Greenland ice sheet mass loss, J. Glaciol., 60, 782–794, doi:10.3189/2014JoG13J202, 2014. 1390

Arthern, R. J. and Gudmundsson, G. H.: Initialization of ice-sheet forecasts viewed as an inverse Robin problem, J. Glaciol., 56, 527–533, doi:10.3189/002214310792447699, 2010. 1389

Bamber, J. L., Layberry, R. L., and Gogenini, S. P.: A new ice thickness and bed data set for the Greenland ice sheet 1: Measurement, data reduction, and errors, J. Geophys. Res., 106, 33773–33780, 2001. 1388

Bindschadler, R. A., Nowicki, S., Abe-Ouchi, A., Aschwanden, A., Choi, H., Fastook, J., Granzow, G., Greve, R., Gutowski, G., Herzfeld, U., Jackson, C., Johnson, J., Khroulev, C.,

SeaRISE revisited

F. Saito et al.

Title Page

Abstract | Introduction

Conclusions | References

Tables | Figures

|◀ | ▶|

◀ | ▶

Back | Close

Full Screen / Esc

Printer-friendly Version

Interactive Discussion

Levermann, A., Lipscomb, W. H., Martin, M. A., Morlighem, M., Parizek, B. R., Pollard, D., Price, S. F., Ren, D., Saito, F., Sato, T., Seddik, H., Seroussi, H., Takahashi, K., Walker, R., and Wang, W. L.: Ice-sheet model sensitivities to environmental forcing and their use in projecting future sea level (the SeaRISE project), J. Glaciol., 59, 195–224, 2013. 1384, 1386, 1387, 1392, 1395, 1400, 1406, 1407, 1409, 1420, 1421

Braithwaite, R. J. and Olesen, O. B.: Calculation of glacier ablation from air temperature, West Greenland, in: Glacier Fluctuations and Climatic Change, edited by: Oerlemans, J., Kluwer Academic Publishers, Dordrecht, 219–233, 1989. 1394

Cuffey, K. M. and Paterson, W. S. B.: The Physics of Glaciers, 4th Edn., Academic Press, Amsterdam, 2010. 1393

Dansgaard, W., Johnsen, S. J., Clausen, H. B., Dahl-Jensen, D., Gudestrup, N. S., Hammer, C. U., Hvidberg, C. S., Steffensen, J. P., Sveinbjörnsdottir, A. E., Jouzel, J., and Bond, G.: Evidence for general instability of past climate from a 250-kyr ice-core record, Nature, 364, 218–220, 1993. 1397

Edwards, T. L., Fettweis, X., Gagliardini, O., Gillet-Chaulet, F., Goelzer, H., Gregory, J. M., Hoffman, M., Huybrechts, P., Payne, A. J., Perego, M., Price, S., Quiquet, A., and Ritz, C.: Effect of uncertainty in surface mass balance–elevation feedback on projections of the future sea level contribution of the Greenland ice sheet, The Cryosphere, 8, 195–208, doi:10.5194/tc-8-195-2014, 2014. 1385, 1410

Ettema, J., van den Broeke, M. R., van Meijgaard, E., van de Berg, W. J., Bamber, J. L., Box, J. E., and Bales, R. C.: Higher surface mass balance of the Greenland ice sheet revealed by high-resolution climate modeling, Geophys. Res. Lett., 36, L12501, doi:10.1029/2009GL038110, 2009. 1394

Fausto, R. S., Ahlstrøm, A. P., As, D. V., Bøggild, C. E., and Johnsen, S. J.: A new present-day temperature parameterization for Greenland, J. Glaciol., 55, 95–105, 2009. 1394

Gillet-Chaulet, F., Gagliardini, O., Seddik, H., Nodet, M., Durand, G., Ritz, C., Zwinger, T., Greve, R., and Vaughan, D. G.: Greenland ice sheet contribution to sea-level rise from a new-generation ice-sheet model, The Cryosphere, 6, 1561–1576, doi:10.5194/tc-6-1561-2012, 2012. 1385

Goelzer, H., Huybrechts, P., Fürst, J., Nick, F., Andersen, M., Edwards, T., Fettweis, X., Payne, A., and Shannon, S.: Sensitivity of Greenland ice sheet projections to model formulations, J. Glaciol., 59, 733–749, doi:10.3189/2013JoG12J182, 2013. 1385, 1390

Title Page

Abstract | Introduction

Conclusions | References

Tables | Figures

|◄ | ►|

◄ | ►

Back | Close

Full Screen / Esc

Printer-friendly Version

Interactive Discussion

Graversen, R., Drijfhout, S., Hazeleger, W., van de Wal, R., Bintanja, R., and Helsen, M.: Greenland's contribution to global sea-level rise by the end of the 21st century, Clim. Dynam., 37, 1427–1442, doi:10.1007/s00382-010-0918-8, 2011. 1385

Greve, R.: On the response of the Greenland ice sheet to greenhouse climate change, Climatic Change, 46, 289–303, 2000. 1394

Greve, R.: Relation of measured basal temperatures and the spatial distribution of the geothermal heat flux for the Greenland ice sheet, Ann. Glaciol., 42, 424–432, 2005. 1397

Greve, R. and Herzfeld, U. C.: Resolution of ice streams and outlet glaciers in large-scale simulations of the Greenland ice sheet, Ann. Glaciol., 54, 209–220, doi:10.3189/2013AoG63A085, 2013. 1385

Greve, R., Saito, F., and Abe-Ouchi, A.: Initial results of the SeaRISE numerical experiments with the models SICOPOLIS and IcIES for the Greenland ice sheet, Ann. Glaciol., 52, 23–30, 2011. 1392, 1397

Herzfeld, U. C., Fastook, J., Greve, R., McDonald, B., Wallin, B. F., and Chen, P. A.: On the influence of Greenland outlet glacier bed topography on results from dynamic ice-sheet models, Ann. Glaciol., 53, 281–293, doi:10.3189/2012AoG60A061, 2012. 1385, 1388

Hindmarsh, R. C. A. and Le Meur, E.: Dynamical processes involved in the retreat of marine ice sheets, J. Glaciol., 47, 271–282, 2001. 1388, 1393

Hutter, K.: Theoretical Glaciology, Material Science of Ice and the Mechanics of Glaciers and Ice Sheets, Springer Netherlands, Dordrecht, 1983. 1393

Huybrechts, P.: The Antarctic ice sheet and environmental change: a three-dimensional modelling study, PhD thesis, Ber. Polarforsch., Alfred Wegener Institute for Polar and Marine Research, Bremerhaven, 1992. 1393

Huybrechts, P. and de Wolde, J.: The dynamic response of the Greenland and Antarctic ice sheets to multiple-century climatic warming, J. Climate, 12, 2169–2188, 1999. 1384, 1385, 1393, 1394, 1399, 1404, 1417, 1422

Huybrechts, P., Letréguilly, A., and Reeh, N.: The Greenland ice sheet and greenhouse warming, Palaeogeogr. Palaeocl., 89, 399–412, 1991. 1385

Huybrechts, P., Janssens, I., Poncin, C., and Fichefet, T.: The response of the Greenland ice sheet to climate changes in the 21st century by interactive coupling of an AOGCM with a thermomechanical ice-sheet model, Ann. Glaciol., 35, 409–415, 2002. 1394

Johnsen, S. J., Clausen, H. B., Dansgaard, W., Gundestrup, N. S., Hammer, C. U., Andersen, U., Andersen, K. K., Hvidberg, C. S., Dahl-Jensen, D., Steffensen, J. P., Shoji, H., Svein-

Title Page

Abstract | Introduction

Conclusions | References

Tables | Figures

|◄ | ►|

◄ | ►

Back | Close

Full Screen / Esc

Printer-friendly Version

Interactive Discussion

bjornsdottir, A. E., White, J., Jouzel, J., and Fisher, D.: The δ^{18}O record along the Greenland Ice Core Project deep ice core and the problem of possible Eemian climatic instability, J. Geophys. Res., 102, 26397–26410, doi:10.1029/97JC00167, 1997. 1397

Nowicki, S., Bindschadler, R. A., Abe-Ouchi, A., Aschwanden, A., Bueler, E., Choi, H., Fastook, J., Granzow, G., Greve, R., Gutowski, G., Herzfeld, U., Jackson, C., Johnson, J., Khroulev, C., Larour, E., Levermann, A., Lipscomb, W. H., Martin, M. A., Morlighem, M., Parizek, B. R., Pollard, D., Price, S. F., Ren, D., Rignot, E., Saito, F., Sato, T., Seddik, H., Seroussi, H., Takahashi, K., Walker, R., and Wang, W. L.: Insights into spatial sensitivities of ice mass response to environmental change from the SeaRISE ice sheet modeling project II: Greenland, J. Geophys. Res.-Earth, 118, 1025–1044, doi:10.1002/jgrf.20076, 2013. 1386, 1390, 1395, 1396, 1407, 1409, 1410

Paterson, W. S. B.: The Physics of Glaciers, 3rd Edn., Pergamon, Oxford, 1994. 1393

Reeh, N.: Parameterization of melt rate and surface temperature on the Greenland ice sheet, Polarforschung, 59, 113–128, 1991. 1392, 1394

Ritz, C., Fabre, A., and Letréguilly, A.: Sensitivity of a Greenland ice sheet model to ice flow and ablation parameters: consequences for the evolution through the last climatic cycle, Clim. Dynam., 13, 11–24, 1997. 1394

Robinson, A., Calov, R., and Ganopolski, A.: Greenland ice sheet model parameters constrained using simulations of the Eemian Interglacial, Clim. Past, 7, 381–396, doi:10.5194/cp-7-381-2011, 2011. 1395

Rogozhina, I., Martinec, Z., Hagedoorn, J. M., Thomas, M., and Fleming, K.: On the long-term memory of the Greenland ice sheet, J. Geophys. Res.-Earth, 116, F01011, doi:10.1029/2010JF001787, 2011. 1385, 1390

Saito, F. and Abe-Ouchi, A.: Sensitivity of Greenland ice sheet simulation to the numerical procedure employed for ice sheet dynamics, Ann. Glaciol., 42, 331–336, 2005. 1392

Seddik, H., Greve, R., Zwinger, T., Gillet-Chaulet, F., and Gagliardini, O.: Simulations of the Greenland ice sheet 100 years into the future with the full Stokes model Elmer/Ice, J. Glaciol., 58, 427–440, doi:10.3189/2012JoG11J177, 2012. 1385

Seroussi, H., Morlighem, M., Rignot, E., Khazendar, A., Larour, E., and Mouginot, J.: Dependence of century-scale projections of the Greenland ice sheet on its thermal regime, J. Glaciol., 59, 1024–1034, doi:10.3189/2013JoG13J054, 2013. 1385, 1390, 1396

Shannon, S. R., Payne, A. J., Bartholomew, I. D., van den Broeke, M. R., Edwards, T. L., Fettweis, X., Gagliardini, O., Gillet-Chaulet, F., Goelzer, H., Hoffman, M. J., Huybrechts, P.,

Title Page

Abstract | Introduction

Conclusions | References

Tables | Figures

|◄ | ►|

◄ | ►

Back | Close

Full Screen / Esc

Printer-friendly Version

Interactive Discussion

Mair, D. W. F., Nienow, P. W., Perego, M., Price, S. F., Smeets, C. J. P. P., Sole, A. J., van de Wal, R. S. W., and Zwinger, T.: Enhanced basal lubrication and the contribution of the Greenland ice sheet to future sea-level rise, P. Natl. Acad. Sci. USA, 110, 14156–14161, doi:10.1073/pnas.1212647110, 2013. 1385

Stone, E. J., Lunt, D. J., Rutt, I. C., and Hanna, E.: Investigating the sensitivity of numerical model simulations of the modern state of the Greenland ice-sheet and its future response to climate change, The Cryosphere, 4, 397–417, doi:10.5194/tc-4-397-2010, 2010. 1392

Tarasov, L. and Peltier, W. R.: Greenland glacial history and local geodynamic consequences, Geophys. J. Int., 150, 198–229, doi:10.1046/j.1365-246X.2002.01702.x, 2002. 1396, 1398, 1399, 1404, 1417, 1422

Yan, Q., Zhang, Z., Gao, Y., Wang, H., and Johannessen, O. M.: Sensitivity of the modeled present-day Greenland Ice Sheet to climatic forcing and spin-up methods and its influence on future sea level projections, J. Geophys. Res.-Earth, 118, 2174–2189, doi:10.1002/jgrf.20156, 2013. 1385, 1389, 1390, 1400

Title Page

Abstract · Introduction

Conclusions · References

Tables · Figures

◄ · ►

◄ · ►

Back · Close

Full Screen / Esc

Printer-friendly Version

Interactive Discussion

Table 1. Summary of all the numerical experiment in this paper. The bedrock column denotes the sources of bedrock topography as boundary condition (see main text for interpretation of symbols). The column "sub-melt" denotes whether or not to sub-melt basal sliding occurrence based on Eq. (3) is implemented. The surface melt column denotes which method is adopted for computation of surface melting or surface mass balance: "T" follows PDD of Tarasov and Peltier (2002), "H" follows PDD of Huybrechts and de Wolde (1999), "S" is with the melting field provided by SeaRISE, respectively. The initialization columns denotes climate forcing used for initializing the ice-sheet topography, where "125 ky tr" stands for 125 kyr transient forcing based on ice-core record, and "0 ka st" stands for steady-state experiment under the present-day condition. Thickness columns denotes how the ice thickness is computed during initialization phase, where "free" means that ice-thickness is allowed to evolve freely, "fixed (obs)" means that ice-thickness kept fixed as the present-day observation through the initialization phase artificially, "fixed (B 0 ka)" and "fixed (B' 0 ka)" mean that ice-thickness kept fixed as the simulated topography at 0 ka obtained by experiments with configuration B and B', respectively. Margin column denotes whether the ice margin is allowed to advance freely (free) or limited to the initial condition (no advance) during future-climate experiments.

Exp.	bedrock	sub-melt	surface melt	initialization	thickness	margin
O	dev1.2	n	T	125 ky tr	free	free
A	JHKP	n	T	125 ky tr	free	free
B	JHKP	y	T	125 ky tr	free	free
D	JHKP	y	T	125 ky tr	fixed (obs.)	free
E	JHKP	y	T	125 ky tr	fixed (obs.)	no advance
B'	JHKP	y	H	125 ky tr	free	free
D'	JHKP	y	H	125 ky tr	fixed (obs.)	free
E'	JHKP	y	H	125 ky tr	fixed (obs.)	no advance
D_s	JHKP	y	T	0 ka st	fixed (obs.)	free
D'_s	JHKP	y	H	0 ka st	fixed (obs.)	free
E_s	JHKP	y	T	0 ka st	fixed (obs.)	no advance
E'_s	JHKP	y	H	0 ka st	fixed (obs.)	no advance
F	JHKP	y	T	125 ky tr	fixed (B0 ka)	free
F'	JHKP	y	H	125 ky tr	fixed (B'0 ka)	free
F_s	JHKP	y	T	0 ka st	fixed (B0 ka)	free
F'_s	JHKP	y	H	0 ka st	fixed (B'0 ka)	free
E''_s	JHKP	y	S	0 ka st	fixed (obs.)	no advance

Table 2. Simulated ice-sheet volume ($\times 10^{15}\,\mathrm{m}^3$) and the ratio (%) relative to the present-day observed volume $2.91 \times 10^{15}\,\mathrm{m}^3$. The volumes of other experiments such as D, E etc are identical to the observed value by definition.

	v1	(%)	v2	(%)	v4	(%)
O	3.08	+5.8	3.00	+3.2	2.93	+0.5
A	3.03	+4.2	2.96	+1.7	2.89	−0.8
B F F$_s$	2.96	+1.7	2.81	−3.4	2.60	−10.6
B$'$ F$'$ F$'_s$	3.08	+5.8	2.95	+1.3	2.79	−4.0

Table 3. Simulated changes in VAF (cm) relative to corresponding constant future climate experiments at 500 years from the present for the configurations B and F and their differences and the two configuration D and D$'$ and their diffrerences.

	C1 − C0			C2 − C0			C3 − C0		
Config.	v1	v2	v4	v1	v2	v4	v1	v2	v4
B	−36.5	−41.8	−53.6	−77.1	−90.2	−108.8	−150.9	−169.2	−185.6
F	−32.4	−38.2	−54.7	−76.0	−91.5	−116.8	−156.0	−177.9	−200.1
B − F	−4.1	−3.7	+1.1	−1.1	+1.3	+8.0	+5.1	+8.7	+14.5
D	−26.0	−27.4	−30.3	−52.6	−56.6	−63.6	−111.6	−120.4	−137.9
D$'$	−19.9	−21.7	−24.8	−39.3	−42.6	−48.6	−74.2	−79.4	−89.3
D − D$'$	−6.1	−5.7	−5.5	−13.3	−14.0	−15.0	−37.3	−41.1	−48.6
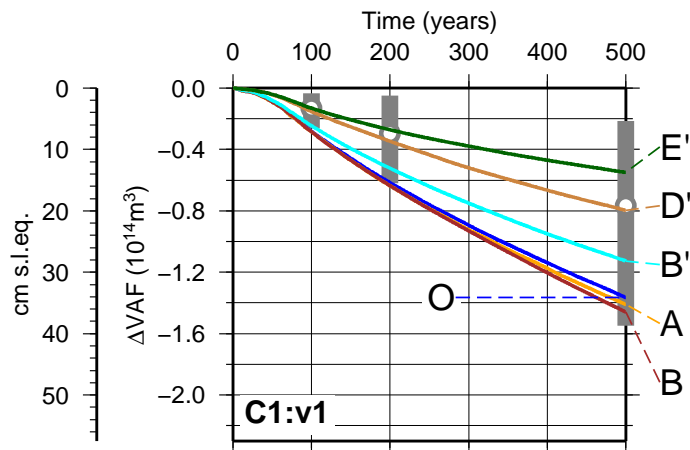
Figure 1. Simulated changes in VAF (volume above flotation, see the main text) obtained by future-climate runs under experimental configuration of `O` (IcIES SeaRISE compatible), `A`, `B`, `B'`, `D'` and `E'`, in terms of the difference relative to the result of corresponding constant-climate experiments (`C0`). The results of `C1` (A1B climate forcing) climate scenario, with "standard" sliding coefficient (`v1`) are shown. The vertical gray bars indicate the range of results summarized in the SeaRISE (Bindschadler et al., 2013, Table 3) at 100, 200 and 500 years. The circles in the gray bars indicate the mean values of all the SeaRISE participants.
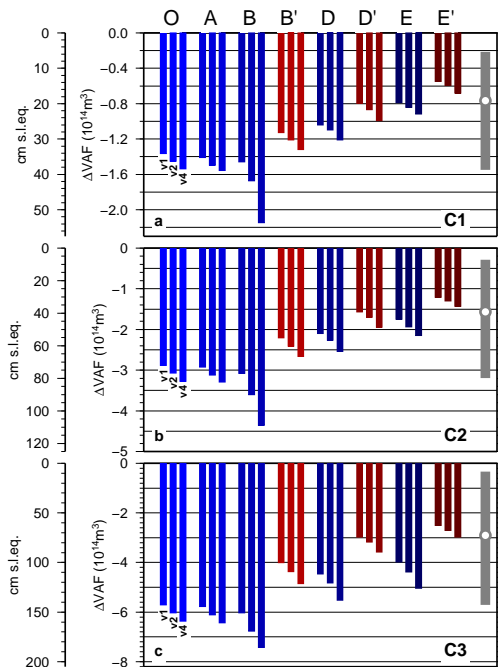
Figure 2. Simulated changes in VAF at 500 years from the present-day obtained by future-climate runs under experimental configuration of O (IcIES SeaRISE compatible), in terms of the difference relative to the result of corresponding constant-climate experiments (C0), under experimental configuration of O (IcIES SeaRISE compatible), A, B, B′, D, D′, E and E′. Three bars from left to right in each configuration correspond to the results for v1 (using "standard" sliding coefficients), v2 (2×) and v4 (4×), respectively. The top, middle and lower panels are results of run C1 (A1B climate forcing), C2 (1.5× A1B) and C3 (2× A1B), respectively. The vertical gray bars at the right indicate the range of results summarized in SeaRISE (Bindschadler et al., 2013, Table 3) at 500 years. The circles in the gray bars indicate the mean values of all the SeaRISE participants.

Title Page

Abstract   Introduction

Conclusions   References

Tables   Figures

|◄   ►|

◄   ►

Back   Close

Full Screen / Esc
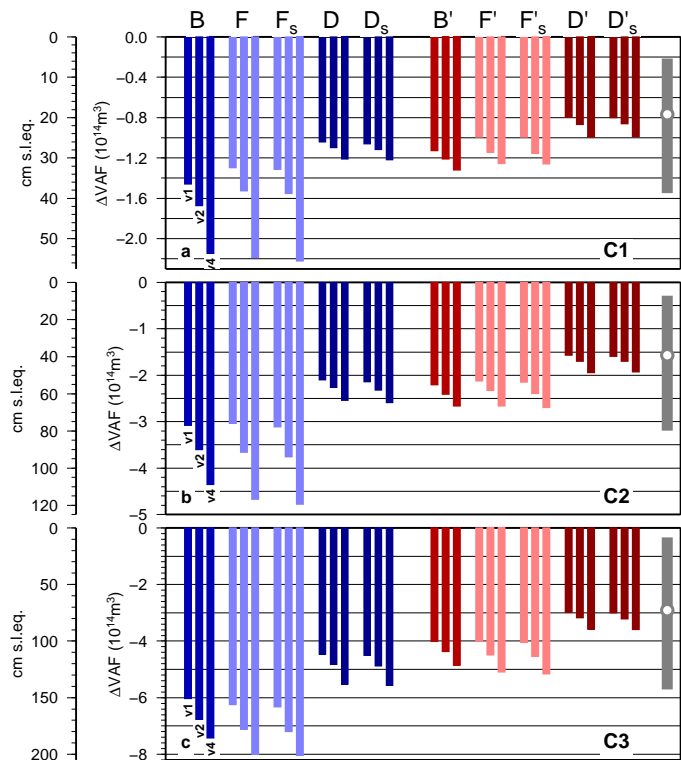
Printer-friendly Version

Interactive Discussion

Figure 3. The same figures as Fig. 2 under experimental configuration of B, F, F_s, D, D_s, B', F', F'_s, D', D'_s, respectively. The left five experiments apply Tarasov and Peltier (2002) while the right five apply Huybrechts and de Wolde (1999) for the surface mass balance computation, respectively.
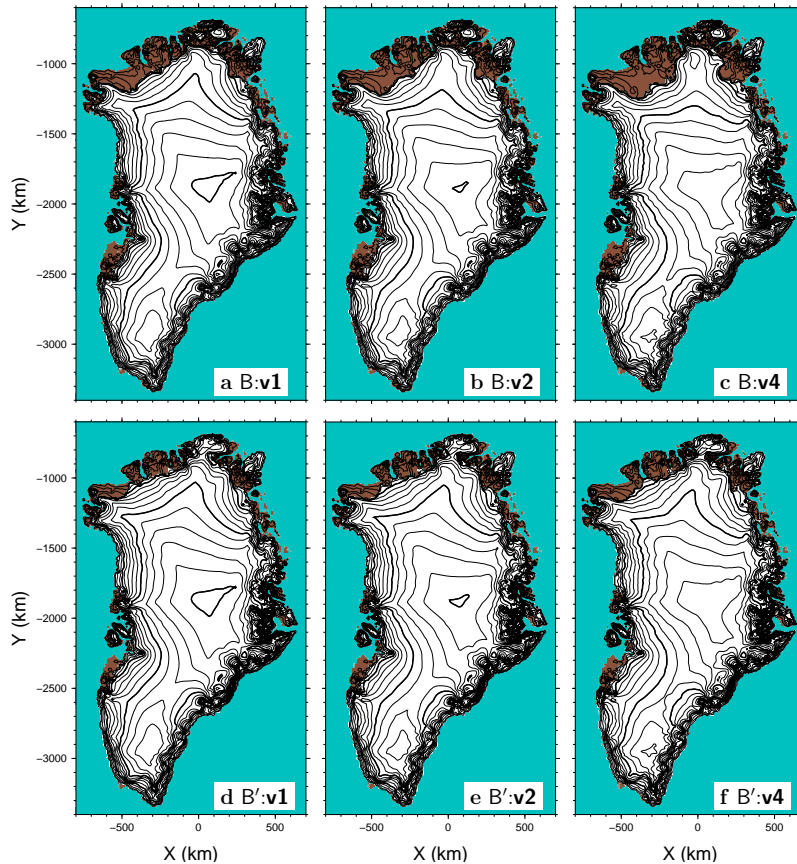
Title Page

Abstract | Introduction

Conclusions | References

Tables | Figures

◄ | ►

◄ | ►

Back | Close

Full Screen / Esc

Printer-friendly Version

Interactive Discussion

Figure 4. Simulated present-day surface topography obtained by experiments with the free spin-up initialization, B (upper panels) and B′ (lower panels). Contour intervals are 200 and 1000 m for thin and thick lines, respectively.
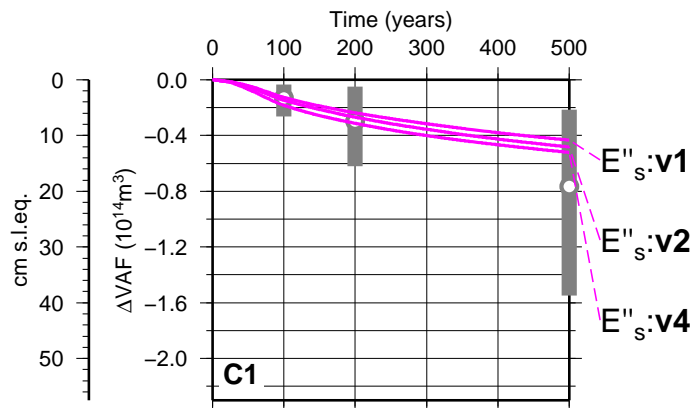
Figure A1. Simulated changes in VAF obtained by future-climate run `C1` under experimental configuration of E''_s using three different sliding coefficient (`v1`, `v2` and `v4`).